Fourier Transform Infrared Spectroscopic Study of the Interactions of a Strongly Antimicrobial but Weakly Hemolytic Analogue of Gramicidin S with Lipid Micelles and Lipid Bilayer Membranes†

Ruthven N. A. H. Lewis, Monika Kiricsi, Elmar J. Prenner, Robert S. Hodges,‡ and Ronald N. McElhaney*

Department of Biochemistry and Protein Engineering Network of Centers of Excellence, University of Alberta, Edmonton, Alberta, Canada T6G 2H7

Received August 22, 2002; Revised Manuscript Received November 12, 2002

ABSTRACT: Cyclo[VKL*d*KV*d*YPLKVKL*d*YP] (GS14*d*K$_4$), a synthetic tetradecameric ring-size analogue of the naturally occurring antimicrobial peptide gramicidin S (GS), retains the strong antimicrobial activity of GS but is 15−20 times less hemolytic. To characterize its interaction with lipid membranes and to understand the molecular basis of its capacity to lyse bacterial cells, in preference to erythrocytes, we have investigated the interactions of GS14*d*K$_4$ with detergent micelles and with lipid bilayer model membranes by Fourier transform infrared spectroscopy and compared our results with those of a similar study of GS [Lewis, R. N. A. H., et al. (1999) *Biochemistry 38*, 15193−15203]. In both aqueous and organic solvent solutions, GS14*d*K$_4$ adopts a β-sheet conformation that is somewhat distorted and more sensitive to the polarity of its environment than GS. Like GS, GS14*d*K$_4$ is completely or partially excluded from gel-state lipid bilayers but interacts strongly with liquid-crystalline lipid bilayers and detergent micelle, and interacts more strongly with more fluid liquid-crystalline lipid systems. However, its interactions are more strongly influenced by membrane lipid order and fluidity, and unlike GS, it is essentially excluded from cholesterol-containing phospholipid bilayers. Also, GS14*d*K$_4$ is excluded from cationic lipid bilayers, but partitions more strongly and/or penetrates more deeply into anionic lipid bilayers than into those composed of either zwitterionic or nonionic lipids. Anionic lipids also facilitate GS14*d*K$_4$ interactions with multicomponent lipid bilayers which are predominantly zwitterionic or nonionic. Although GS14*d*K$_4$ generally penetrates and/or partitions into zwitterionic or uncharged lipid bilayers less strongly than does GS, its greater size and altered distribution of positive charges make it intrinsically more perturbing with regard to membrane organization once associated with lipid bilayers. This fact, combined with its relatively strong interactions with anionic phospholipids, may explain why GS14*d*K$_4$ retains relatively high antimicrobial activity. However, its low hemolytic activity is probably largely attributable to its low propensity to penetrate and/or partition into cholesterol-containing zwitterionic lipid membranes.

Gramicidin S (GS),[1] a cyclic decapeptide of primary structure [cyclo(Val-Orn-Leu-D-Phe-Pro)$_2$], was first isolated from *Bacillus brevis* (*1*) and is one of a series of antimicrobial peptides produced by this microorganism (*2*, *3*). GS exhibits strong antibiotic activity against a broad spectrum of both Gram-negative and Gram-positive bacteria, as well as against several pathogenic fungi (*4*−*7*). However, GS also exhibits appreciable hemolytic activity, and as a result, its potential use as an antibiotic is restricted to topical applications (*8*). However, recent work has shown that structural analogues of GS can be designed with comparable antimicrobial activity but markedly reduced hemolytic activity, suggesting the possibility that appropriate GS derivatives might in principle be used as potent oral or injectable broad-spectrum antibiotics (*4*−*7*).

There have been numerous studies of the relationship between the chemical structure of GS analogues and their antimicrobial and hemolytic activities (see refs *2* and *3*). Unfortunately, in most cases, these two activities vary more or less in parallel. However, by altering both the size of the

† Supported by operating and major equipment grants from the Canadian Institutes of Health Research, by major equipment grants from the Alberta Heritage Foundation for Medical Research, and by an operating grant from the Protein Engineering Network of Centers of Excellence. M.K. was supported in part by a Hungarian Eötvös Fellowship.

* To whom correspondence should be addressed. Telephone: (780) 492-2413. Fax: (780) 492-0095. E-mail: rmcelhan@gpu.srv.ualberta.ca.

‡ Present address: Department of Biochemistry and Molecular Genetics, University of Colorado Health Sciences Center, Denver, CO 80262.

[1] Abbreviations: GS, gramicidin S, cyclo[VOL*d*FPVOL*d*FP] (the amino acid immediately after *d* is the D-enantiomer); GS14, cyclo[VKLKV*d*YPLKVKL*d*YP]; GS14*d*K$_4$, cyclo[VKL*d*KV*d*YPLKVKL*d*YP]; PC, phosphatidylcholine; PE, phosphatidylethanolamine; PG, phosphatidylglycerol; PS, phosphatidylserine; DMPC, dimyristoylphosphatidylcholine; DEPC, dielaidoylphosphatidylcholine; SOPC, 1-stearoyl-2-oleoylphosphatidylcholine; DMPE, dimyristoylphosphatidylethanolamine; DMPG, dimyristoylphosphatidylglycerol; DMPS, dimyristoylphosphatidylserine; TMCL, tetramyristoylcardiolipin; DE-MGDG, dielaidoyl monoglucosyldiacylglycerol; DE-DGDG, dielaidoyl diglucosyldiacylglycerol; Et-DMPC, P-O-ethyl dimyristoylphosphatidylcholine; FTIR, Fourier transform infrared; NMR, nuclear magnetic resonance; DSC, differential scanning calorimetry; CD, circular dichroism; T_m, hydrocarbon chain melting phase transition temperature; TFE, trifluoroethanol; CTAB, cetyl trimethylammonium bromide; SDS, sodium dodecyl phosphate; L_β, lamellar gel phase; L_α, lamellar liquid-crystalline phase; T_m, lamellar/gel/liquid-crystalline phase transition temperature.

10.1021/bi026707a CCC: $25.00
Published on Web 12/17/2002

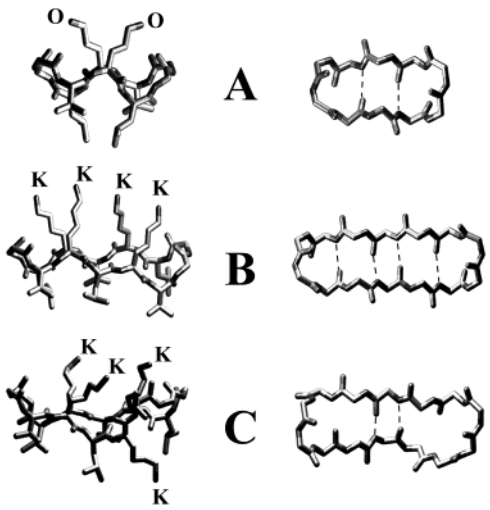

FIGURE 1: Molecular models of the antimicrobial peptides GS (A), GS14 (B), and GS14dK_4 (C). The left panel shows side views of the peptide backbone and the orientations of the lysine (K), ornithine (O), and hydrophobic (unlabeled) side chains relative to the ring plane. The right panel shows top views of the peptide backbone with the dashed lines representing connectivities where the distance and orientation of the amide carbonyls and amide protons are favorable for cross-ring hydrogen bonding. The GS and GS14 models that are shown were obtained from minimized structures published by Gibbs et al. (*26*). The GS14dK_4 model was obtained from the NMR solution structures (30% trifluoroethanol) published by McInnes et al. (*11*).

GS ring system and the orientation of amino acid side chains relative to the ring plane by specific enantiomeric (L to D) substitutions, Hodges and co-workers have shown that a dissociation of the antimicrobial and hemolytic activities of GS analogues is possible (*5*, *6*, *9*). A particularly promising peptide which has been identified through this approach is GS14dK_4, a cyclic tetradecamer with antimicrobial potency comparable to that of GS but which is 15−20-fold less hemolytic. This analogue consists of two antiparallel aligned sequences of alternating hydrophobic and cationic residues (Val-Lys-Leu-*d*Lys-Val and Leu-Lys-Val-Lys-Leu) connected at each end of the ring by the dipeptide sequence *d*Tyr-Pro. It is thus a diastereomeric analogue of GS14 in which a D- for L-amino acid substitution occurs at Lys-4. Unlike GS14 itself, where all four Lys side chains occur on the same side of the ring, the Lys-4 side chain of GS14dK_4 projects partially onto the normally completely hydrophobic face of the molecule (see Figure 1). The GS14dK_4 molecule is thus more water soluble, less amphiphilic, and less inclined to aggregate in aqueous solution or to interact strongly with hydrophobic surfaces than is GS14 (*10*). Also, CD and ^{1}H-NMR studies have shown that GS14dK_4 forms a less rigid β-sheet structure which is considerably more sensitive to the polarity and hydrogen bonding capacity of the environment than is GS14, due at least in part to a disruption of cross-ring intramolecular hydrogen bonding by the Lys-4 enantiomeric substitution (*10*, *11*).

The mechanistic basis of the propensity of GS14dK_4 to lyse bacterial cells in preference to erythrocytes, is not understood, and a clear correlation between its physicochemical properties in solution and its capacity to discriminate between microbial and mammalian cells has not been established. Moreover, although the lipid bilayer of the cell membrane is the primary target of this peptide, little is known about the interaction of GS14dK_4 with the lipids of bacterial or animal cell membranes. In this study, we utilize FTIR spectroscopy to characterize the interactions of GS14dK_4 with various detergent micelles and with single-component and multicomponent model membranes to obtain a better understanding of its interactions with membrane lipids and of its ability to discriminate between microbial and animal cell membranes.

MATERIALS AND METHODS

The cyclic peptide GS14dK_4 was synthesized and purified using the methodology described by McInnes et al. (*11*) and converted to the hydrochloride salt by two cycles of lyophilization from 10 mM hydrochloric acid. Commercially available lipids were obtained from Avanti Polar Lipids Inc. (Alabaster, AL) and used without further purification. Elaidate-homogeneous *Acholeplasma laidlawii* membrane lipids were prepared by extracting the polar lipid fraction from cells cultured in avidin-containing, elaidate-supplemented medium using the methodology initially described by Silvius and McElhaney (*12*). DE-MGDG and DE-DGDG were isolated and purified from the aforementioned membrane lipid extracts using methods described by McMullen et al. (*13*). FTIR spectroscopy was performed on both dried films and liquid-based samples. The dried samples were examined as thin films cast from a methanolic solution. Liquid-based samples were prepared as follows. Lipid-free samples containing 0.2−0.5 mg of peptide or lipid-containing samples containing peptide and 1−2 mg of lipid were dissolved or dispersed in the appropriate solvent, and the solution or paste was then squeezed between the CaF_2 windows of a heatable liquid cell (equipped with a Teflon spacer) to form a 25 μm film. Once the cell had been mounted in the sample holder of the instrument, the sample temperature could be regulated between −20 and 90 °C by an external, computer-controlled circulating water bath. With lipid-containing samples, the peptide and lipid were codissolved in methanol to obtain a lipid:peptide ratio of 25:1, and the solvent was removed with a stream of nitrogen and subsequent overnight evacuation. Next, the mixture was hydrated by the addition of 75−100 μL of a D_2O buffer containing 50 mM phosphate and 100 mM NaCl (pH 7.4) followed by vigorous vortexing at temperatures well above the gel−liquid-crystalline phase transition of the lipid. The dispersion so formed was used as described above.

Infrared spectra were recorded with a Digilab FTS-40 infrared spectrometer (Digilab, Cambridge, MA) using data acquisition parameters comparable to those described by Mantsch et al. (*14*). The spectra that were obtained were analyzed and plotted with software supplied by Digilab Inc. and other computer programs obtained from the National Research Council of Canada and from OriginLab Corp. (Northampton, MA). With PS-containing samples, the headgroup carboxylate gives rise to a strong absorption band between 1610 and 1670 cm^{-1} which can effectively mask the contours of the amide I absorption band of the peptide (*15*). For such samples, the compensation for the interference from the carboxylate function was achieved by the application of a weighted spectral subtraction procedure in which the spectra of the pure lipid sample are normalized to the integrated intensity of the lipid C═O stretching band of the peptide-containing sample before subtraction. This procedure

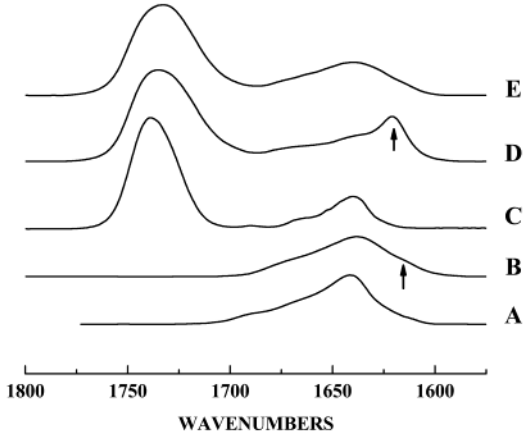

FIGURE 2: FTIR spectra of the amide I bands of GS14*d*K$_4$. Absorbance spectra are presented for (A) a methanol-dried GS14*d*K$_4$ film, (B) unbuffered D_2O solutions of GS14*d*K$_4$, (C) methanol-dried films of a SOPC/GS14*d*K$_4$ mixture (25:1), (D) a D_2O-hydrated SOPC/GS14*d*K$_4$ (25:1) film at gel phase temperatures, and (E) a D_2O-hydrated SOPC/GS14*d*K$_4$ (25:1) film at fluid phase temperatures. The arrows indicate the position of the low-frequency amide I components centered near or below 1620 cm^{-1}.

could only be applied to spectra obtained at temperatures well above and well below the gel−liquid-crystalline phase transition of the lipid/peptide mixture. The procedure works because the presence of the peptide does not alter the shape of the PS ester C═O absorption bands observed at temperatures well above and well below the gel−liquid-crystalline phase transition of the mixture. Aqueous dispersions of the lipid-containing samples used for FTIR spectroscopy were also studied by differential scanning calorimetry to examine the thermotropic phase behavior of the samples actually used for FTIR spectroscopy. Residual material from lipid-containing FTIR spectroscopic samples was diluted with buffer to obtain lipid concentrations near 1.0 mg/mL, and 325 μL aliquots were analyzed with a Nano-DSC high-sensitivity instrument (Calorimetry Sciences Corp., Spanish Fork, UT) operating at heating and cooling rates near 10 °C/h. The data that were obtained were analyzed and plotted with the Origin software package (OriginLab Corp.).

RESULTS

FTIR Spectroscopy of Dried Films and Solutions of GS14dK$_4$. Amide I bands of representative FTIR spectra exhibited by various preparations of GS14*d*K$_4$ are illustrated in Figure 2, and the amide I band maxima of these and other preparations are listed in Table 1. Methanol-dried films of GS14*d*K$_4$ alone exhibit amide I bands which contain a dominant peak centered near 1642 cm^{-1} with smaller components centered between 1660 and 1680 cm^{-1} (Figure 2A), frequencies close to those exhibited by GS under comparable conditions (*16*). In principle, the lower-frequency component, which accounts for at least 70% of the total integrated amide I intensity, could be due to proteated proteins or peptides forming antiparallel β-sheets (*17*−*19*) or to deuterium-exchanged proteins or peptides in helical and/or random-coil conformations (*19*). However, both CD and ^{1}H NMR spectroscopic studies indicate that GS14*d*K$_4$ exists primarily as β-sheets in both aqueous and organic solvents (*10*, *11*), and as noted above, GS14*d*K$_4$ amide I band frequencies are close to those of GS, which exists exclusively as antiparallel β-sheets (see ref *16* and references therein). We therefore assign the main lower-frequency component to the amide I vibrations of the internally hydrogen-bonded residues forming the antiparallel β-sheet portion of the GS14*d*K$_4$ molecule. The other components probably arise mainly from the amide I vibrations of the proline and tyrosine residues forming the type II′ β-turns of the peptide (*16*) and are not the focus of this work.

Table 1: Amide I Band Maxima of the Hydrochloride Salt of GS14*d*K$_4$

sample	band maxima (cm^{-1})	comments
GS14*d*K$_4$	1642	CH_3OH-dried film
GS14*d*K$_4$	1637, 1618[a]	D_2O solution (unbuffered)[b]
GS14*d*K$_4$	1631	PO_4 buffer in D_2O (pD 7.4)[b]
GS14*d*K$_4$	1642	CH_3OD solution[b]
GS14*d*K$_4$	1651, 1664[a]	DMSO solution
DEPC and GS14*d*K$_4$	1640	CH_3OH-dried film
DEPC and GS14*d*K$_4$	1620, 1635[a]	D_2O-hydrated film, gel phase[b]
DEPC and GS14*d*K$_4$	1639	D_2O-hydrated film, fluid phase[b]

[a] Band appears as a shoulder on the main peak. [b] Samples with deuterium-exchanged amide hydrogens.

As expected, the amide I band frequencies of this peptide are strongly influenced by the local environment. A comparison of the amide I frequencies observed with GS14*d*K$_4$ in deuterated aqueous media (∼1631−1637 cm^{-1}), in CH_3OD (∼1642 cm^{-1}), and in dimethyl sulfoxide (∼1651 cm^{-1}) indicates that an appreciable upward shift in amide I band frequency occurs as both the polarity and hydrogen bonding capacity of the solvent decrease. These frequencies and frequency shifts are comparable to the solvent-induced changes observed in our previous FTIR spectroscopic studies of GS (*16*). When GS14*d*K$_4$ is dissolved in deuterated aqueous media, the frequency of its main amide I band (1631−1637 cm^{-1}) is lower than that observed in aqueous media, consistent with the expected downward shift in amide I frequency which occurs upon N-deuteration of the amide bonds of proteins and peptides (*20*−*22*). However, as illustrated in Figure 2B, the amide I band envelope exhibited by D_2O solutions of GS14*d*K$_4$ also contains a low-frequency component centered near 1618 cm^{-1} which accounts for a small but significant fraction (∼20%) of the integrated intensity of the main amide I band near 1635 cm^{-1}. This low-frequency component probably arises from a population of GS14*d*K$_4$ molecules which is conformationally distinct from that predominantly found in GS14*d*K$_4$ dissolved in either TFE or methanol. This band is of interest here because its frequency is well below that expected from N-deuteration of the β-sheet portion of this peptide (see above) and because it appears as a major component only when GS14*d*K$_4$ is associated with a gel-phase lipid (see below).

Methanol-dried mixed films of PC/GS14*d*K$_4$ mixtures exhibit amide I band maxima at frequencies between 1635 and 1638 cm^{-1} (Figure 2C), a range comparable to that observed with methanol-dried films of GS14*d*K$_4$ alone. Upon hydration with deuterated aqueous media and subsequent cooling to temperatures well below the lipid T_m, a low-frequency amide I component centered near 1620 cm^{-1} appears as the dominant feature of the amide I band envelope, accounting for 50−60% of the total integrated amide I intensity (Figure 2D). This low-frequency band seems to be similar to the minor low-frequency amide I component which

Table 2: Amide I Band Maxima of GS14*d*K$_4$ in Deuterated Aqueous Detergents

detergent	band maxima (cm^{-1})	comments
SDS	1642	anionic micelles
CTAB	1632	cationic micelles
octyl glucoside	1639	nonionic micelles
Brij-58	1639	nonionic micelles
1-O-18:0 lyso PC	1640	zwitterionic micelles, at ≥30 °C
1-O-18:0 lyso PC	1633, 1618[a]	zwitterionic coagel, at ≤10 °C

[a] Band appears as a shoulder on the main peak.

is observed in aqueous solutions of GS14*d*K$_4$, and its prominence under these conditions suggests that this conformationally distinct population of GS14*d*K$_4$ molecules is being stabilized by the interaction with the gel phase lipid (see below). At temperatures well above the lipid T_m, the intensity of the low-frequency component diminishes markedly and a broad amide I band envelope emerges near 1639−1640 cm^{-1} (Figure 2E), frequencies higher than those exhibited by GS14*d*K$_4$ in deuterated aqueous media. As previously noted with GS (*16*), the upward shift in amide I frequency accompanying the lipid L_β−L_α phase transition is consistent with the movement of the peptide from a highly polar environment to less polar one such as the polar−apolar interfaces of lipid bilayers. Moreover, this process is accompanied by the disappearance of the conformationally distinct GS14*d*K$_4$ population which is stabilized by its interaction with the gel phase lipid. The amide I band changes noted above are thus the combined result of a lipid phase state-induced decline of this latter GS14*d*K$_4$ population and the migration of GS14*d*K$_4$ molecules into the polar−apolar interfacial regions of the lipid bilayer.

GS14dK$_4$ in Detergent Micelles. The amide I band frequencies exhibited by GS14*d*K$_4$ in deuterated aqueous solutions of cationic, anionic, and nonionic detergents are summarized in Table 2. When codissolved in buffer with the cationic detergent CTAB, GS14*d*K$_4$ exhibits amide I frequencies near 1632 cm^{-1}, values essentially the same as those observed in the aqueous buffer, indicating that significant interaction with cationic CTAB micelles is unlikely. In contrast, the amide I frequencies observed when GS14*d*K$_4$ is codissolved with anionic, nonionic, and zwitterionic detergent micelles are some 7−10 cm^{-1} higher than those observed in buffer alone. This observation indicates that GS14*d*K$_4$ resides in a less polar environment than the bulk aqueous phase and implies that significant GS14*d*K$_4$ penetration or partitioning into the anionic, nonionic, and zwitterionic detergent micelles occurs. Also, the amide I frequencies observed when GS14*d*K$_4$ interacts with SDS micelles are somewhat higher than those observed when the peptide interacts with the nonionic and zwitterionic detergents that were examined (see Table 2), consistent with greater partitioning and/or a deeper penetration of this peptide into the anionic detergent micelles.

Interactions of GS14dK$_4$ with Single-Component Lipid Bilayers. Figure 3A shows a stacked plot of the temperature-dependent changes in the lipid C═O stretching and peptide amide I regions of the infrared spectra exhibited by aqueous dispersions of a DMPC/GS14*d*K$_4$ (25:1) mixture. At low temperatures, the dominant feature of the amide I absorption band of GS14*d*K$_4$ is a relatively sharp major component

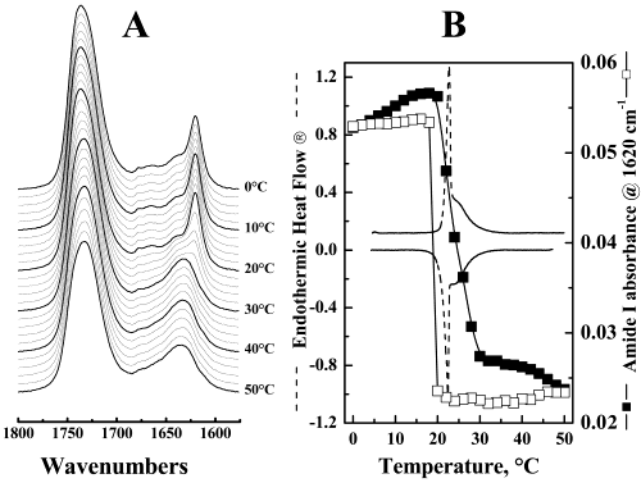

FIGURE 3: Interaction of GS14*d*K$_4$ with DMPC model membranes. (A) Stacked plot illustrating the temperature-dependent changes in the C═O stretching and amide I regions of FTIR spectra exhibited by an aqueous dispersion of a 25:1 mixture of DMPC and GS14*d*K$_4$. The absorbance spectra that are shown were acquired between 0 and 50 °C. (B) Temperature-dependent changes in the intensity of the sharp low-frequency amide I component of the infrared spectra exhibited by aqueous dispersions of DMPC/GS14*d*K$_4$ mixtures (25:1). Plots are shown for data acquired in the heating (■) and cooling (□) mode. DSC heating and cooling thermograms of the same mixture are included to demonstrate the correspondence between the appearance and disappearance of this spectroscopic feature relative to the onset and completion of the gel−liquid-crystalline phase transition of the lipid/peptide mixture.

centered near 1620 cm^{-1}. Once heating has taken place, this feature persists with undiminished intensity to temperatures near the onset of the membrane L_β−L_α phase transition, and its intensity decreases progressively as the phase transition proceeds. Upon completion of the membrane L_β−L_α phase transition, the low-frequency amide I band disappears completely and the amide I band envelope consists of a broad peak centered near 1637−1640 cm^{-1} (see Figure 3A). The thermally induced changes in the features of the GS14*d*K$_4$ amide I band are fully reversed upon cooling (Figure 3B). However, unlike in the heating mode, the broad amide I features characteristic of the L_α phase persist to temperatures coincident with the lower boundary of the cooling exotherm, and with further cooling, an abrupt reappearance of the sharp, low-frequency amide I component occurs. These observations strongly suggest that the sharp low-frequency amide I component centered near 1620 cm^{-1} is correlated with the predominance of the gel phase lipid. This possibility was examined by a study of PC/GS14*d*K$_4$ mixtures in which the T_m was incrementally varied by changes in the length of the lipid hydrocarbon chains.

Illustrated in Figure 4 are temperature-dependent changes in peptide amide I intensity at 1620 cm^{-1} and the calorimetrically determined normalized heat capacity integrals exhibited by mixtures of GS14*d*K$_4$ with various members of the homologous series of *n*-saturated PCs. The data presented therein reveal two very important features. First, the temperature ranges over which the sharp, low-frequency amide I component disappears upon heating generally increase with increases in lipid hydrocarbon chain length, suggesting that the observed thermally induced changes in the features of the peptide amide I band are the result of its association with the lipids and are not attributable to

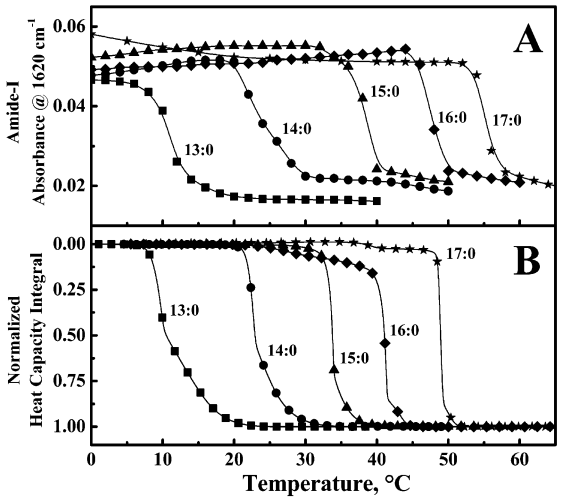

FIGURE 4: Effect of hydrocarbon chain length on the temperature-dependent changes in the intensities of GS14*d*K$_4$ amide I absorption at 1620 cm^{-1} (A) and in the normalized heat capacity integrals (B) exhibited by mixtures of GS14*d*K$_4$ with phosphatidylcholine bilayers. Normalized heat capacity integrals were obtained by integrating the DSC heating thermograms of the various samples and dividing the integrals by the total area obtained. Data are presented for mixtures of GS14*d*K$_4$ with 13:0 PC (■), 14:0 PC (●), 15:0 PC (▲), 16:0 PC (◆), and 17:0 PC (★).

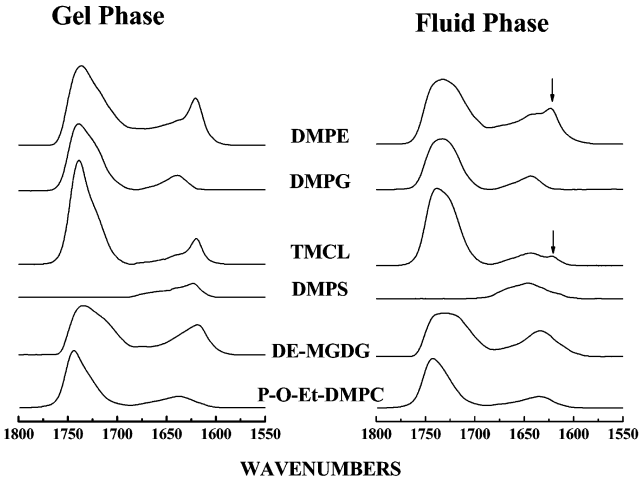

FIGURE 5: Representative spectra showing the C═O stretching and amide I regions of the infrared spectra exhibited by a 25:1 mixture of GS14*d*K$_4$ with the indicated phospholipid and glycolipid bilayers. The data are typical of those obtained at temperatures 10 °C below (gel phase) and 5 °C above (fluid phase) the onset and completion, respectively, of the lipid gel−liquid-crystalline phase transitions of the various lipid/peptide mixtures. The arrows mark the positions of residual low-frequency components which persist in the liquid-crystalline phases of the DMPE- and TMCL-based mixtures. The amide I bands of the DMPS/GS14*d*K$_4$ mixtures were obtained by spectral subtraction as described in Materials and Methods.

temperature changes alone. Second, a comparison of the temperature-dependent changes in the peptide amide I band with those of the normalized heat capacity integrals (Figure 4B) indicates that the disappearance of the peptide low-frequency amide I component does not always coincide with the $L_\beta-L_\alpha$ phase transition of the lipid. For example, when mixed with 13:0 PC bilayers, the decrease in the intensity of the low-frequency amide I band begins upon heating to temperatures slightly below the onset of the $L_\beta-L_\alpha$ phase transition of the lipid/peptide mixture and is essentially complete at temperatures some 3−4 °C below the completion of the $L_\beta-L_\alpha$ phase transition. With the 14:0 PC/GS14*d*K$_4$ mixture, the temperature range spanned by the disappearance of the low-frequency amide I band essentially coincides with the onset and completion of the lipid $L_\beta-L_\alpha$ phase transition as determined from the normalized heat capacity integrals (Figure 4B) or from the temperature-dependent changes in the symmetric CH_2 stretching band of the PC hydrocarbon chains (data not shown). With further increases in lipid hydrocarbon chain length, the temperature range spanned by the disappearance of the low-frequency amide I component is progressively shifted upward relative to the onset and completion of the $L_\beta-L_\alpha$ phase transition and may even begin at temperatures above the completion of the $L_\beta-L_\alpha$ phase transition of the mixture (see Figure 4A). The tendency for such changes to be initiated at temperatures somewhat above the completion of the $L_\beta-L_\alpha$ phase transitions of mixtures containing longer chain PCs was also observed when the peptide was incorporated into bilayers composed of the unsaturated lipids SOPC and DEPC (data not shown). This pattern of behavior differs markedly from that observed in comparable studies of GS/PC mixtures (*16*). These observations suggest that the observed changes in the GS14*d*K$_4$ amide I band may not be directly triggered by changes in the phase state of the host lipid bilayer per se. The implications and possible physical basis of this observation will be examined later.

Illustrated in Figure 5 are FTIR spectra which typify those obtained at temperatures below and above the onset and completion temperatures of mixtures of GS14*d*K$_4$ with PE and with the other types of single-component model membranes that have been examined. These lipid/peptide mixtures do not exhibit hydrocarbon chain length-dependent behavior comparable to that described above for the PC/GS14*d*K$_4$ mixtures. At temperatures below the onset of the lipid $L_\beta-L_\alpha$ phase transition, PE/GS14*d*K$_4$ mixtures exhibit amide I absorption bands which contain a sharp dominant component centered near 1620 cm^{-1}, a feature similar to that observed with PC/GS14*d*K$_4$ mixtures. Once heating has taken place, the sharp low-frequency band persists with undiminished intensity until the onset of the $L_\beta-L_\alpha$ phase transition and decreases markedly in intensity as the temperature increases through and above the $L_\beta-L_\alpha$ phase transition. Concomitant with the decline in the intensity of the low-frequency amide I band is the growth of a broader amide I component centered near 1637 cm^{-1}. However, unlike the PC/GS14*d*K$_4$ mixtures, the sharp low-frequency amide I band remains as a significant component of the amide I band contour at temperatures at least 40 °C above the completion of $L_\beta-L_\alpha$ phase transition of the mixture, though a slow progressive decline in its intensity continues upon further heating. The persistence of this component at elevated temperatures suggests that in contrast to PC bilayers, a sizable fraction of the added peptide does not penetrate and/or partition into liquid-crystalline PE bilayers. This result contrasts sharply with our previous studies of GS wherein essentially quantitative partitioning into liquid-crystalline PE bilayers was observed at higher temperatures (*16*).

Figure 5 also shows evidence for a different pattern of interactions of GS14*d*K$_4$ with anionic lipid bilayers. For example, the PG-based lipid/peptide mixtures do not exhibit the sharp low-frequency amide I component described above. At temperatures below the onset of the $L_\beta-L_\alpha$ phase

transition of this lipid/peptide mixture, the amide I band is centered near 1638 cm^{-1}, and coincident with the melting of the lipid hydrocarbon chains, its frequency drifts upward to values near 1644−1646 cm^{-1}, behavior comparable to that observed when GS is incorporated into PG bilayers (*16*). Once cooling has taken place, a downward shift in the amide I frequency begins at temperatures near the completion of the L_β−L_α phase transition and is essentially complete at temperatures 5−10 °C below the lower boundaries of the calorimetrically detected cooling exotherm (data not shown). The absence of the sharp low-frequency amide I component at low temperatures markedly differentiates these spectroscopic observations from those of GS14*d*K$_4$ mixtures with zwitterionic lipids and strongly suggests that the membrane interactions which stabilize the conformationally distinct GS14*d*K$_4$ population do not occur when the peptide is associated with PG bilayers. However, the frequency of the amide I band maxima observed at temperatures well below the T_m of this lipid/peptide mixture is higher than that observed in aqueous solution. This observation suggests that there are also interactions between GS14*d*K$_4$ and the gel phases of PG bilayers, but that these interactions are not conducive to the stabilization of the peptide conformation which gives rise to the low-frequency peak mentioned above. Finally, the L_β−L_α phase transition of the GS14*d*K$_4$/PG mixture is accompanied by an increase in the frequency of the amide I band to frequencies near 1644 cm^{-1}. These values are higher than those observed when GS14*d*K$_4$ interacts with the L_α phases of either PC or PE bilayers and suggest that this peptide interacts more strongly with the L_α phase of the anionic lipid.

Interestingly, we also find that the spectroscopic characteristics exhibited by PG/GS14*d*K$_4$ mixtures are not typical of the interaction of this peptide with other anionic lipid bilayers. As illustrated in Figure 5, mixtures of GS14*d*K$_4$ with the anionic lipids TMCL and DMPS both exhibit a sharp, low-frequency amide I band near 1620 cm^{-1} comparable to what is observed with PC- and PE-based mixtures. Moreover, once heating to temperatures well above their respective L_β−L_α phase transitions had taken place, the intensity of this lower-frequency component diminishes with the concomitant emergence of a broader amide I band contour centered at frequencies near 1644−1645 cm^{-1} (Figure 4). Evidently, the spectroscopic behavior of the GS14*d*K$_4$/TMCL and GS14*d*K$_4$/PS mixtures is more comparable to that exhibited by mixtures of GS14*d*K$_4$ with PC bilayers. However, the amide I frequencies observed at temperatures well above the L_β−L_α phase transitions of the TMCL- and PS-based mixtures are some 4−6 cm^{-1} higher than those observed with the PC-based mixtures, consistent with greater partitioning and/or deeper penetration into the TMCL and PS bilayers in the liquid-crystalline state. We also note that with the TMCL-based mixtures, the sharp low-frequency component persists with undiminished intensity until the onset of the lipid L_β−L_α phase transition and, although its intensity progressively declines as the transition progresses, does not disappear completely until temperatures some 10 °C above the completion of the transition (see Figure 5). This pattern of behavior is also unlike that observed with the PG-based mixtures but is remarkably similar to that observed when GS14*d*K$_4$ is with 15:0 and 16:0 PC (see Figure 4).

The infrared spectroscopic changes in the amide I bands accompanying the L_β−L_α phase transitions of mixtures of GS14*d*K$_4$ with the nonionic glycolipid DE-MGDG (Figure 5) are essentially similar to those exhibited by mixtures of GS14*d*K$_4$ and DE-DGDG. At temperatures below the L_β−L_α phase transition, the amide I bands consist of a somewhat skewed band envelope with a peak centered near 1620 cm^{-1}. Once heating to temperatures well above the lipid T_m has taken place, the amide I band adopts a more symmetrical shape with its peak centered near 1634 cm^{-1}, changes that are fully reversible upon cooling. These spectroscopic changes are also the result of a phase state-induced decline in the intensity of an amide I component near 1620 cm^{-1} and a concomitant increase in the intensity of a broader component centered near 1634 cm^{-1}. In general, these changes are qualitatively similar to those which occur when GS14*d*K$_4$ interacts with PC bilayers and with anionic bilayers composed of TMCL and PS. However, the amide I frequencies observed when the peptide interacts with the L_α phases of these nonionic bilayers are somewhat lower than those observed when it interacts with bilayers composed of PC and especially of the anionic lipids that have been studied, suggesting that the interaction of GS14*d*K$_4$ with the L_α phase of these nonionic bilayers is probably weaker than is the case with bilayers composed of any of the zwitterionic and anionic phospholipids.

Finally, unlike all of the other lipid/peptide mixtures that have been examined, GS14*d*K$_4$ mixtures with the cationic lipid P-O-Et-DMPC exhibit a broad amide I band envelope centered near 1633−1635 cm^{-1}, the peak frequency of which is essentially insensitive to changes in the temperature and phase state of the host lipid bilayers (see Figure 5), suggesting that GS14*d*K$_4$ may not be interacting with P-O-Et-DMPC bilayers. This suggestion is consistent with the absence of peptide-induced broadening of the lipid L_β−L_α phase transition as monitored by DSC (data not shown). In this respect, the behavior of GS14*d*K$_4$ differs markedly from that of GS, for which there is evidence of peptide partitioning into liquid-crystalline P-O-Et-DMPC bilayers at higher temperatures (*16*). Also, in contrast to the other lipid/peptide mixtures studied except those with PG, Et-DMPC/GS14*d*K$_4$ mixtures do not exhibit a sharp low-frequency amide I component at temperatures below the lipid L_β−L_α phase transition. Evidently, the gel phase membrane interactions which stabilize the GS14*d*K$_4$ population which gives rise to the sharp low-frequency amide I component near 1620 cm^{-1} do not occur with P-O-Et-DMPC bilayers.

Interactions of GS14dK$_4$ with Multicomponent Lipid Bilayers. The interactions of GS14*d*K$_4$ with a number of lipid mixtures were examined to study how the interactions of GS14*d*K$_4$ are likely to be affected by the lipid headgroup compositional heterogeneity which typifies natural cell membranes. Figure 6A illustrates the C═O stretching and amide I regions of the infrared spectra exhibited by a mixture of *A. laidlawii* B membrane lipids with GS14*d*K$_4$ at temperatures well above and well below its L_β−L_α phase transition. When cultured under our conditions, *A. laidlawii* membrane polar lipids are composed of the nonionic glycolipids MGDG and DGDG (60−70 mol %), PG (20−30 mol %), and smaller quantities of other anionic species such as phosphorylated glycolipids and aminoacylated phosphatidylglycerols (*23*). At low temperatures, the mixture of *A.*

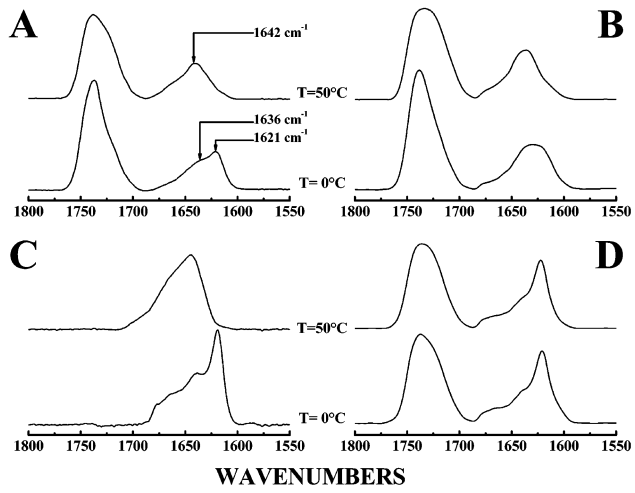

FIGURE 6: C═O stretching and amide I regions of infrared spectra exhibited by mixtures of GS14*d*K_4 with various lipid mixtures. The absorbance spectra that are shown typify data acquired in the gel (low temperature) and fluid (high temperature) phases of the mixtures. Data are presented for mixtures of GS14*d*K_4 with (A) elaidate-homogeneous *A. laidlawii* B membrane lipids, (B) DEPE and DEPG (7:3), (C) DEPC, DEPE, and DEPS (1:1:1), and (D) DMPC membranes containing 30 mol % cholesterol. The spectra in panel C are estimates of the amide contours of GS14*d*K_4 obtained by spectral subtraction as described in Materials and Methods.

laidlawii polar lipids with GS14*d*K_4 exhibits an amide I band envelope which contains a relatively small sharp component centered near 1620 cm^{-1} and a broader component centered near 1636 cm^{-1} (Figure 6, panel A). Once heating had taken place, both components begin to diminish in intensity at temperatures just below the onset of the $L_\beta-L_\alpha$ phase transition and, upon completion of the phase transition, are replaced by a single broader component centered near 1642 cm^{-1}. These spectroscopic changes are fully reversible upon cooling, albeit with a temperature hysteresis of some 3−4 °C (data not shown). The latter frequency is slightly lower than that seen when GS14*d*K_4 interacts with liquid-crystalline PG bilayers but much higher than that observed when the peptide interacts with the nonionic glycolipids (see Figure 5), suggesting that its interaction with the L_α phases of these multicomponent bilayers is stronger than is the case with those composed of each of the pure glycolipid components but weaker than with those composed of PG alone. This result thus provides evidence for PG facilitation of stronger GS14*d*K_4−membrane interactions.

PG-facilitated GS14*d*K_4−membrane interaction is also apparent when the peptide interacts with PE/PG (7:3) model membranes (model mimetic for the cell membranes of Gram-negative bacteria such as *Escherichia coli*). GS14*d*K_4 exhibits a broad amide I band envelope centered near 1629 cm^{-1} when it interacts with the gel phases of these PE/PG membranes and a slightly narrower band envelope centered near 1638 cm^{-1} at temperatures well above the $L_\beta-L_\alpha$ phase transition temperatures of those membranes (Figure 6B). Further analyses indicate that the broad amide I band observed at low temperatures is actually a summation of comparably intense components centered near 1620 and 1634 cm^{-1}. Once heating has taken place, the 1620 cm^{-1} component progressively diminishes in intensity as the lipids melt and is replaced by a component centered near 1642 cm^{-1} which coexists with the amide I component centered near 1634 cm^{-1}. These spectroscopic results differ markedly from those observed when the peptide interacts with membranes composed of PE alone (see Figure 5).

The amide I band contours exhibited when GS14*d*K_4 interacts with bilayers composed of equimolar amounts of PC, PE, and PS (model mimetic for the cell membrane lipid compositions of yeasts and many other fungi) are shown in Figure 6B. At temperatures well below the $L_\beta-L_\alpha$ phase transition, there exists a sharp amide I component centered near 1620 cm^{-1}, similar to what is observed when the peptide interacts with each of the pure lipid components alone. However, at temperatures well above the T_m of the mixture, the GS14*d*K_4 amide I band is centered near 1640−1642 cm^{-1}, values below those observed when the peptide partitions into liquid-crystalline PS bilayers but above those observed when the peptide interacts with liquid-crystalline bilayers composed of either PC or PE alone. Evidently PS, like PG, is capable of facilitating GS14*d*K_4−membrane interaction.

The effect of GS14*d*K_4 on cholesterol-containing PC membranes was also examined to estimate its probable interactions with the cholesterol-containing, predominantly zwitterionic membranes which occur on the outer surfaces of mammalian cells. Mixtures of GS14*d*K_4 with DMPC membranes containing 30 mol % cholesterol exhibit amide I band envelopes that are dominated by the sharp amide I component (∼1620 cm^{-1}) which typifies the interaction of this peptide with most gel phase lipid bilayers (see Figure 6D). This amide I feature persists to temperatures well above the broad thermotropic phase transitions characteristic of cholesterol-containing PC membranes (for an example of the latter, see ref *24*), and our spectral subtraction analyses indicate that there is a <10% decline in its relative intensity between −2 and 75 °C (data not shown). These results differ markedly from those observed when GS14*d*K_4 interacts with membranes composed of PC alone (see Figure 4), suggesting that the presence of cholesterol drastically inhibits the interaction of GS14*d*K_4 with liquid-crystalline PC bilayers. Moreover, the magnitude of this inhibition is considerably larger than that observed when GS interacts with cholesterol-containing PC membranes, where significant GS penetration of cholesterol-containing PC membranes occurs at temperatures above the membrane T_m (*25*). These results are of special significance given the low hemolytic activity of GS14*d*K_4 relative to that of GS (*6*, *9*).

DISCUSSION

The conformational stability of GS14*d*K_4 and its sensitivity to the properties of the local environment of the peptide are important considerations in the interpretation of the spectroscopic data presented here. The enantiomeric substitution at Lys-4 destabilizes the stable β-sheet structure of GS14 by disrupting the cross-ring intramolecular hydrogen bonding (for more information about the structure of GS14, see refs *5*, *6*, and *26*). Thus, GS14*d*K_4 is not as conformationally stable as either GS14 or GS, and unlike the latter peptides, its solution structure is dependent upon the polarity of the solvent (*10*, *11*). In these FTIR spectroscopic studies, we find that the β-sheet structures formed when GS14*d*K_4 crystallizes from a methanolic solution exhibit amide I absorption bands at frequencies near 1642 cm^{-1}, some 7−9 cm^{-1} higher than those exhibited by GS [∼1735 cm^{-1} (*16*)]

and GS14 [~1733 cm^{-1} (unpublished data from this laboratory)] under comparable conditions. The higher amide I frequencies observed with GS14*d*K$_4$ probably arise because of the nonideal β-sheet H-bonding geometry due to the destabilization of the GS14 structure by the enantiomeric substitution at Lys-4.

Aqueous solutions of GS14*d*K$_4$ exhibit FTIR spectra suggesting the existence of at least two populations of GS14*d*K$_4$ molecules. This observation is compatible with the results of a recent ^{1}H-NMR spectroscopic study, which suggests that GS14*d*K$_4$ exists as a mixture of distorted β-sheet structures (major population) and relatively "unstructured" conformations (minor population) in aqueous solution (*11*). This NMR spectroscopic study also showed that some induction of structure occurs upon transfer of GS14*d*K$_4$ from water to TFE, and although distorted β-sheet structures remain the dominant conformational motifs in TFE solution, their conformations were not the same as those existing in water (*11*). Those results are compatible with recent CD data which also show some induction of structure when lipid vesicles are mixed with aqueous solutions of GS14*d*K$_4$ (*27*). In this study, we demonstrate that upon association with aqueous lipid micelles or liquid-crystalline lipid bilayers, GS14*d*K$_4$ exhibits amide I frequencies that are higher than those observed in aqueous media, consistent with the migration of the peptide from a relatively polar environment to a less polar one (*16*). However, given the results of previous CD and ^{1}H-NMR spectroscopic studies, a conformational change in GS14*d*K$_4$ may also contribute to the observed amide I frequency changes. In this respect, the behavior of GS14*d*K$_4$ differs markedly from that of conformationally stable peptides such as GS and GS14, for which the amide I frequency shifts observed in comparable FTIR spectroscopic studies arise exclusively from changes in the polarity of the local environment of the peptide (*16*). Nevertheless, the conformational changes in GS14*d*K$_4$ are expected to be relatively minor since distorted β-sheet structures are the dominant conformational motifs present in both water and membrane mimetic media (*11*). Thus, with GS14*d*K$_4$, we also assign these amide I frequency changes primarily to the effect of transferring the peptide from water to a less polar environment within the lipid assembly (most probably the lipid polar−apolar interfacial region). The magnitude of the various frequency changes observed upon interaction with liquid-crystalline lipid bilayers relative to that observed in water is thus interpreted primarily in terms of variations in the relative strength of the interactions between GS14*d*K$_4$ and the various lipids that have been studied.

An unusual aspect of the data presented is the reversible appearance of a sharp low-frequency amide I component (1615−1620 cm^{-1}) as a major feature of the GS14*d*K$_4$ amide I band envelope when various lipid/GS14*d*K$_4$ mixtures are cooled to temperatures well below the T_m. The occurrence of the low-frequency amide I component was not surprising because a GS14*d*K$_4$ amide I component in this frequency range is present in the infrared spectra of GS14*d*K$_4$ in D_2O solution (see Figure 2). When GS14*d*K$_4$ is dissolved in unbuffered deuterated aqueous solvents, the low-frequency amide I band typically comprises a relatively small fraction (~20%) of the integrated intensity of the amide I band envelope and its intensity does not change significantly with changes in temperature. However, with most lipid/GS14*d*K$_4$ mixtures, this component is a major feature of the amide I band envelope, comprising some 70% the total integrated amide I intensity at temperatures below the onset of the L_β−L_α phase transition. Once heating has taken place, the intensity of this component begins to diminish at temperatures near the L_β−L_α phase transition, and in most cases, it disappears completely when the lipids convert to the L_α phase. The formation of the GS14*d*K$_4$ population which gives rise to this low-frequency amide I component thus seems to be promoted by its interactions with well-ordered lipid bilayers. In principle, this low-frequency band could be due to the aggregation of peptide β-sheets (see ref *19* and references therein). However, aggregation of this peptide seems unlikely because aggregated protein or peptide β-sheets usually exhibit a pair of sharp amide I absorption bands centered near 1618 and 1680 cm^{-1} (*19*), and because previous studies provide no evidence for aggregation of this peptide when it is dissolved in aqueous buffers at concentrations comparable to those used in this study (*10*). Moreover, the appearance of this band is a fully reversible process which is generally linked to the membrane L_β−L_α phase transition, whereas the aggregation of protein β-sheets is generally irreversible. Thus, we tentatively assign the sharp low-frequency amide I component to a conformationally distinct GS14*d*K$_4$ population which is formed in aqueous solution and stabilized by interaction with gel-state lipid bilayers. The conformation of this form of the peptide and the nature of its association with gel-state lipid bilayers are both unknown at this time. However, since cell membranes normally contain only liquid-crystalline lipid, this form of the peptide is unlikely to be relevant to its mode of action. Nevertheless, its appearance provides a useful and easily identifiable indicator for the existence of lipid-associated GS14*d*K$_4$ populations which have not partitioned into lipid membranes.

Table 3: Amide I Band Maxima in the Liquid-Crystalline Phases of Hydrated GS14*d*K$_4$/Lipid Mixtures

membrane lipid	band maxima (cm^{-1})	comments
PC	1640	zwitterionic
PE	1639, 1618[a]	zwitterionic
PS	1645	anionic
PG	1644	anionic
TMCL	1644	anionic, at ≥50 °C
DE-MGDG	1633	nonionic, at ≥40 °C
DE-DGDG	1633	nonionic, at ≥40 °C
P-O-Et-DMPC	1635	cationic, at ≥30 °C
PE and PG (7:3)	1642	
PC, PE, and PS (1:1:1)	1644	
A. laidlawii B membrane lipids	1643, 1636	
PC and cholesterol (7:3)	1620	zwitterionic

[a] Band appears as a shoulder on the main peak.

A survey of the amide I frequencies observed in the liquid-crystalline states of the various lipid/GS14*d*K$_4$ mixtures that have been examined (see Table 3) reveals that in those cases where GS14*d*K$_4$ interacts with single-component model membranes, the observed amide I frequencies decrease in the following order: anionic membranes > zwitterionic membranes > nonionic membranes ~ cationic membranes. A similar pattern of behavior is also observed when GS14*d*K$_4$ interacts with detergent micelles. Given that increases in the GS14*d*K$_4$ amide I frequency are associated primarily with a

decrease in the polarity of its environment (Table 1), these results can thus be interpreted in terms of either variations in the lipid−water partition coefficient of the peptide, variations in the depth of the penetration of GS14*d*K_4 into the lipid membranes, or both. Distinguishing between these two mechanisms would require more precise information about how variations in membrane lipid composition affect both the location of GS14*d*K_4 in lipid membranes and its lipid−water partitioning than can be gleaned from studies of this type. Nevertheless, both interpretations are consistent with anionic lipids facilitating stronger GS14*d*K_4 interaction with liquid-crystalline lipid bilayers, as has been observed in previous studies of GS−membrane interactions (*16*), and in other studies of interactions between cationic antimicrobial peptides and lipid membranes (*28*−*30* and references therein).

It is clear that the interactions which are relevant to the antimicrobial and hemolytic activities of GS14*d*K_4 occur exclusively in the L_α phases of lipid membranes. Interestingly, with a number of the GS14*d*K_4/lipid mixtures that have been examined, the formation of liquid-crystalline lipid is not sufficient for the peptide to penetrate and/or partition into the membrane, and in most of those instances, further thermal disordering of the host lipid membrane is necessary for either the initiation or completion of the process. In principle, this observation can be rationalized by suggesting that membrane fluidity is also an important determinant of the capacity of GS14*d*K_4 to penetrate and/or partition into the L_α phases of lipid membranes. This suggestion is consistent with the tendency of this peptide to interact more extensively with the L_α phases of PG and PC bilayers which are ostensibly more disordered than those derived from PE and MGDG. More significantly, however, the influence of membrane fluidity can explain why GS14*d*K_4 is essentially excluded from cholesterol-containing PC bilayers at temperatures well above the T_m. It is well-known that cholesterol decreases the fluidity and increases hydrocarbon chain orientational order in liquid-crystalline lipid bilayers (see ref *31* and references therein). This ordering effect of cholesterol can easily explain our results, as well as the tendency for cholesterol to attenuate the potentially deleterious effects of GS and other membrane-disruptive peptides (*25*, *32*−*36*).

Finally, it is interesting to compare the differing patterns of the interactions between GS14*d*K_4 and GS with lipid model membranes and their differential capacities for disrupting bacterial and erythrocyte membranes. As discussed above, both peptides interact more strongly with anionic than with zwitterionic or uncharged lipid membranes and more strongly with more disordered and more fluid lipid bilayers than with membranes that are more ordered and less fluid. However, in all the systems that have been studied, the interaction of GS14*d*K_4 with such model membranes is generally weaker than GS itself, and the differences between the strengths of their interactions are greatest with cationic bilayers, intermediate with zwitterionic or uncharged bilayers, and smallest with anionic bilayers. We ascribe these latter observations to the higher cationic charge of GS14*d*K_4 (+4) relative to that of GS (+2). The weaker interaction of GS14*d*K_4 with model membranes in general is probably due a combination of its greater solubility in water (*10*), which would reduce its tendency to partition into the lipid phase, and its reduced amphiphilic character (*10*), which would reduce its affinity for the polar−apolar interfacial regions of lipid bilayers, the preferred location for GS binding (*28*). Moreover, because GS14*d*K_4 is larger than GS, its insertion into the polar−apolar interfacial regions of lipid bialyers may not be as energetically favorable, because its greater size would make it intrinsically more disruptive to membrane cohesion. This suggestion is supported by the observation that despite its apparently weaker interactions with lipid model membranes, GS14*d*K_4 is actually more effective at permeabilizing cholesterol-free model membranes than is GS (*27*). The larger size of GS14*d*K_4 and its generally weaker interaction with lipid bilayers may also explain why its interactions with membrane lipids are more sensitive to the membrane lipid order and fluidity, as is manifest most dramatically here by its virtual exclusion from cholesterol-containing phospholipid bilayers. We therefore suggest that despite its weaker interactions with lipids in general, GS14*d*K_4 retains the ability to kill bacteria as effectively as GS because of the combination of its higher selectivity for the anionic lipids present in bacterial membranes and its stronger tendency to disrupt lipid bilayers once inserted. Similarly, we ascribe the weaker hemolytic activity of GS14*d*K_4 to its weaker interaction with the zwitterionic phospholipids present on the outer lipid monolayer of the erythrcyte membrane, and to the fact that unlike bacterial membranes, the red cell membrane is highly enriched in cholesterol.

REFERENCES

1. Gause, G. G., and Brazhnikova, M. G. (1944) *Nature 154*, 703.
2. Izumiya, N., Kato, T., Aoyaga, H., Waki, M., and Kondo, M. (1979), *Synthetic Aspects of Biologically Active Cyclic Peptides: Gramicidin S and Tyrocidines*, Halsted Press, New York.
3. Waki, M., and Izumiya, N. (1990) in *Biochemistry of Peptide Antibiotics: Recent Advances in the Biotechnology of β-Lactams and Microbial Bioactive Peptides* (Kleinkauf, H., and van Doren, H., Eds.) Walter de Gruyter and Co., Berlin.
4. Kondejewski, L. H., Farmer, S. W., Wishart, D., Kay, C. M., Hancock, R. E. W., and Hodges, R. S. (1996) *Int. J. Pept. Protein Res. 47*, 460−466.
5. Kondejewski, L. H., Farmer, S. W., Wishart, D., Kay, C. M., Hancock, R. E. W., and Hodges, R. S. (1996) *J. Biol. Chem. 271*, 25261−25268.
6. Kondejewski, L. H., Jelokhani-Niaraki, M., Farmer, S. W., Lix, B., Kay, C. M., Sykes, B. D., Hancock, R. E. W., and Hodges, R. S. (1999) *J. Biol. Chem. 274*, 13181−13192.
7. Jelokhani-Niaraki, M., Kondejewski, L. H., Farmer, S. W., Hancock, R. E. W., Kay, C. M., and Hodges, R. S. (2000) *Biochem. J. 349*, 747−755.
8. Lambert, H. P., and O'Grady, F. W. (1992) *Antibiotic and Chemotherapy*, pp 232−233, Churchill Livingstone, Edinburgh, Scotland.
9. Kondejewski, L. H., Lee, D. L., Jelokhani-Niaraki, M., Farmer, S. W., Hancock, R. E., and Hodges, R. S. (2002) *J. Biol. Chem. 277*, 67−74.
10. Jelokhani-Niaraki, M., Prenner, E. J., Kondejewski, L. H., Kay, C. M., McElhaney, R. N., and Hodges, R. S. (2001) *J. Pept. Res. 58*, 293−306.
11. McInnes, C., Kondejewski, L. H., Hodges, R. S., and Sykes, B. D. (2000) *J. Biol. Chem. 275*, 14287−14297.
12. Silvius, J. R., and McElhaney, R. N. (1978) *Can. J. Biochem. 56*, 462−469.
13. McMullen, T. P. W., Wong, B. C. M., Tham, E. L., Lewis, R. N. A. H., and McElhaney, R. N. (1996) *Biochemistry 35*, 16789−16798.
14. Mantsch, H. H., Madec, C., Lewis, R. N. A. H., and McElhaney, R. N. (1985) *Biochemistry 24*, 2440−2446.
15. Lewis, R. N. A. H., and McElhaney, R. N. (2000) *Biophys. J. 79*, 2043−2055.

16. Lewis, R. N. A. H., Prenner, E. J., Kondejewski, L. H., Flach, C. R., Mendelsohn, R., Hodges, R. S., and McElhaney, R. N. (1999) *Biochemistry 38*, 15193−15203.
17. Arrondo, J. L. R., Muga, A., Castresana, J., and Goni, F. (1993) *Prog. Biophys. Mol. Biol. 59*, 23−56.
18. Jackson, M., and Mantsch, H. H. (1995) *Crit. Rev. Biochem. Mol. Biol. 30*, 95−120.
19. Tamm, L. S., and Tatulian, S. A. (1997) *Q. Rev. Biophys. 30*, 365−429.
20. Pinchas, S., and Laulicht, I. (1971) *Infrared spectra of labeled compounds*, Academic Press, London.
21. Dwivedi, A. M., and Krimm, S. (1982) *Macromolecules 15*, 177−185.
22. Dwivedi, A. M., and Krimm, S. (1982) *Macromolecules 15*, 186−193.
23. Silvius, J. R., Mak, N., and McElhaney, R. N. (1980) *Biochim. Biophys. Acta 597*, 199−215.
24. McMullen, T. P. W., Lewis, R. N. A. H., and McElhaney, R. N. (1993) *Biochemistry 32*, 516−522.
25. Prenner, E. J., Lewis, R. N. A. H., Jelokhani-Niaraki, M., Hodges, R. S., and McElhaney, R. N. (2001) *Biochim. Biophys. Acta 1510*, 83−92.
26. Gibbs, A. C., Kondejewski, L. H., Gronwald, W., Nip, A. M., Hodges, R. S., Sykes, B. D., and Wishart, D. D. (1998) *Nat. Struct. Biol. 5*, 284−288.
27. Jelokhani-Niaraki, M., Prenner, E. J., Kay, C. M., McElhaney, R. N., and Hodges, R. S. (2002) *J. Pept. Res. 60*, 23−36.
28. Prenner, E. J., Lewis, R. N. A. H., and McElhaney, R. N. (1999) *Biochim. Biophys. Acta 1462*, 201−221.
29. Sitaramn, N., and Nagaraj, R. (1999) *Biochim. Biophys. Acta 1462*, 29−54.
30. Shai, Y. (1999) *Biochim. Biophys. Acta 1462*, 55−70.
31. McMullen, T. P. W., and McElhaney, R. N. (1996) *Curr. Opin. Colloid Interface Sci. 1*, 83−90.
32. Christensen, Fink, B. J., Merrifeld, R. B., and Mauzerall, D. (1988) *Proc. Natl. Acad. Sci. U.S.A. 85*, 5072−5076.
33. Maloy, W. L., and Kari, U. P. (1995) *Biopolymers 37*, 105−122.
34. Tytler, E. M., Anantharamaiah, G. M., Walk, D. E., Mishra, V. K., Palgunachari, M. N., and Segrest, J. P. (1995) *Biochemistry 34*, 4393−4401.
35. Matsuzaki, K., Sugishita, K., Fujii, N., and Miyajima, K. (1995) *Biochemistry 34*, 3423−3429.
36. Silvestro, L., Gupta, K., Weiser, J. N., and Axelsen, P. H. (1997) *Biochemistry 36*, 11452−11460.

BI026707A